

## ACCELERATING THE USAGE OF EARTH AND OCEANS OBSERVATION DATA IN HYDROGRAPHIC APPLICATIONS

The Canadian Hydrographic Service

By René Chénier\*, Khalid Omari, Enrique Blondel, Mesha Sagram  
and Adam Jirovec

\* Corresponding author.



### Abstract

Accessing accurate, up-to-date data to support chart production in Canada's vast and complex waterways can be challenging. In order to improve efficiency in charting these navigable waters, The Canadian Hydrographic Service (CHS) has developed new techniques that leverage Satellite Based Earth Observation (EO) data. The main applications developed by CHS include: Satellite Derived Bathymetry (SDB), intertidal zone mapping, extraction of accurate coastlines, change detection/rate of change of coastal features and virtual tidal gauges. The results obtained demonstrate that EO data is a reliable source of Hydrosatial information that can meet the CHS and International Hydrographic Organization (IHO) charting requirements.

**Keywords :** Optical Imagery, Radar, Canadian Hydrographic Service, Satellite Derived Bathymetry, Coastline Extraction, Change Detection, InSAR, Polarimetry, Nautical Charts.



### Résumé

Accéder à des données exactes et à jour en vue de soutenir la production de cartes dans les vastes et complexes voies navigables du Canada peut représenter un défi. Afin d'améliorer l'efficacité dans la cartographie de ces eaux navigables, le Service hydrographique canadien (SHC) a développé de nouvelles techniques qui exploitent les données d'observation de la Terre (EO) par satellite. Les principales applications développées par le SHC comprennent : la bathymétrie par satellite (SDB), la cartographie de la zone intertidale, l'extraction de lignes de côte précises, la détection des changements/le taux de changement des caractéristiques côtières et les marégraphes virtuels. Les résultats obtenus montrent que les données EO sont une source fiable d'informations hydrospatiales qui peuvent répondre aux exigences en matière de cartographie du SHC et de l'Organisation hydrographique internationale (OHI).

**Mots clés :** Imagerie optique, radar, Service hydrographique canadien, bathymétrie par satellite, extraction de lignes de côte, détection des changements, InSAR, polarimétrie, cartes marines.



## Resumen

El acceso a datos precisos y actualizados para apoyar la producción de cartas de las vastas y complejas vías fluviales de Canadá puede ser un desafío. Para mejorar la eficacia al cartografiar estas aguas navegables, el Servicio Hidrográfico Canadiense (CHS) ha desarrollado nuevas técnicas que utilizan datos de la Observación de la Tierra (EO) por satélite. Las principales aplicaciones desarrolladas por el CHS incluyen: Batimetría satelital (SDB), cartografía de zonas inter-mareales, extracción de líneas de costa precisas, detección de cambios/nivel de cambios de características costeras y mareógrafos virtuales. Los resultados obtenidos demuestran que los datos de OE son una fuente fidedigna de información hidroespacial que puede cumplir los costeras y mareógrafos virtuales. Los resultados obtenidos demuestran que los datos de OE son una fuente fidedigna de información hidroespacial que puede cumplir los requisitos cartográficos del CHS y de la Organización Hidrográfica Internacional (OHI).

**Palabras clave :** Imágenes ópticas, Radar, Servicio Hidrográfico Canadiense, Batimetría satelital, Extracción de líneas de costa, Detección de cambios, InSAR, Polarimetría, Cartas náuticas.

## 1. Introduction

The Canadian Hydrographic Service (CHS) is the national Hydrographic Office (HO) which is responsible for aiding mariners with safe navigation through Canadian waters. This mandate is supported through the provision of nearly one thousand nautical charts and hundreds of publications which identify risks to navigation in Canada's vast coastal regions, as well as many of its inland waterways. Like all HO's, CHS relies upon traditional hydrographic techniques for the maintenance of its charts, such as multibeam bathymetric surveys, as well as airborne and ground-based Light Detection and Ranging (LiDAR) surveys. While these techniques provide accurate and reliable measurements, their high-cost and limited geographic coverage restrict the ability for wide area application within reasonable periods of time. As Canada contains the longest coastline in the world, significant resources are required to ensure that all navigable waters are charted appropriately and to modern standards. These efforts are amplified in the Arctic as the remoteness and climatic conditions of this region increase the cost of hydrographic surveys and prevent most activities from taking place for the majority of the year.

The Government of Canada has utilized several initiatives to address the challenges of charting to modern standards. Under the World-Class Tanker Safety System Initiative (WCTSS), (Government of Canada, World-Class Tanker Safety System, 2015), and in collaboration with Transport Canada (TC); Fisheries and Oceans Canada (DFO), through the Canadian Coast Guard (CCG) and CHS were responsible for developing the Northern Low Impact Shipping Corridors initiative (Chénier et al., 2016). The work on defining navigational corridors is now continuing under the Oceans Protection Plan (OPP) (Government of Canada, Oceans Protection Plan, 2017). For CHS, this framework helps prioritize its survey and charting efforts in the key navigational areas of the country. This is done with the help of a Geographic Information System (GIS) called the CHS Priority Planning Tool (CPPT), which uses the corridors as one of the primary GIS layers to define CHS surveying and charting priorities (Chénier et al., 2018). Under WCTSS and OPP, new investments were made to increase the safety to navigation in Canadian waters. These investments not only supported an increase in hydrographic survey collection and production of navigational products, but also included the installation of multibeam sonar on CCG vessels for future surveying capabilities. Despite these latest efforts, important gaps still remain to complete coverage of all Canadian waterways. The Canadian Arctic is the region of the country with the most gaps, where only 14% of the waters are adequately surveyed.

To help further develop the safety to navigation and improve survey mission planning, CHS has also been exploring new technologies and modern Hydrosatial tools (Hains, 2020) within remote sensing. Under the Government Related Initiatives Program (GRIP) of the Canadian Space Agency (CSA), CHS has been investigating the potential of Space Based Earth Observation (EO) for various hydrographic applications. This paper will focus on the development of the approaches that were developed by CHS to accelerate and optimize the usage of SBEO. The approaches developed include: (1) Satellite Derived Bathymetry (SDB), (2) Coastline extraction, (3) Evaluation of rates of change, (4) Intertidal zone mapping, and (5) Virtual tidal gauges. These approaches used hybrid solutions that leveraged the advantages of both optical and radar EO sensors while using medium to high resolution imagery. The primary goals of developing these techniques were: (1) evaluate how the different remote sensing techniques could help CHS better meet its mandate and objectives; (2) test these techniques in Canadian waters to get a realistic assessment of their accuracy; and (3) integrate into CHS operations the SBEO techniques that show an adequate level of reliability based on International Hydrographic Organization (IHO) standards.

## 2. EO Dataset

This paper outlines a resume of all SBEO hydrographic applications that were implemented by CHS. Since varying requirements were needed for each application, a multitude of EO sensors were used. For some applications, a hybrid solution that used both optical and radar imagery was implemented. The sensors varied from medium to high resolution. **Table 1.** provides an overview of the sensors used in this research. The sensor type, spatial resolution, spectral resolution, swath and the revisit period are the main factors that influenced the choice of the best sensor to use for each application.

**Table 1:** List of the main EO sensors used in CHS hydrographic applications

Sensor	Type	Resolution				
		Spatial	Spectral Bands	Radiometric	Swath	Temporal
Worldview	Optical	0.5m-High	8 Multispectral (2.5m) 1 Panchromatic (0.5m)	16 bits	16.4 km	1.1 days
Pléiades	Optical	0.5m-High	4 Multispectral (2.8m) 1 Panchromatic (0.5m)	16 bits	20km	26 days
SPOT 6 & 7	Optical	1.5m-High	4 Multispectral (6m) 1 Panchromatic (1.5m)	16 bits	60km	6 tasking plans per day
PlanetScope	Optical	3.6m-High	4 Multispectral	16 bits	24x8km	Daily
RapidEye	Optical	5m-Medium	5 Multispectral	12 bits	77km	Daily (off nadir) 5.5 days (at nadir)
GeoEye-1	Optical	0.5m-High	4 Multispectral (1.65m) 1 Panchromatic (0.41m)	16 bits	15.2km	Sun Synchronous
Sentinel-2	Optical	10m Medium	13 Multispectral (4 bands at 10m)	12 bits	100km	2-3 days (mid latitude)
Landsat	Optical	30m Medium	8 Multispectral (30m) 1 Panchromatic (15m)	16 bits	185x180km	16 days
Radarsat-2	Radar	6m High	Full Polarimetric	SLC	50 km	23 days
		1m High	Spotlight	SLC	18 km	23 days
RCM	Radar	5m	Compact Polarimetry	SLC	30 km	4 times /day
Sentinel-1	Radar	10m	TOPS Dual VV-VH	SLC	250 km	4 days
ALOS	Radar	5m	Dual HH-HV	SLC	70 km	14 days
TerraSar	Radar	3m	HH	SLC	30 km	11 days

The selection of an adequate sensor is dependent on many factors based on the application. For shoreline mapping, the scale of the chart is a good indicator for the image resolution that will be required. **Table 2** shows the Electronic Navigational Charts (ENC) scales based on Navigational Purpose (IHO, S-66, January 2018). Since the mapping standard is approximately half a millimeter at chart scale, the EO requirement for a berthing scale chart at 1:4000 would be 2 m, which would illustrate the need for high resolution data. For harbor scale charts, high resolution data would also be preferable, whereas medium resolution data would be acceptable for approach and coastal charts. The main reason for not using high resolution imagery for all the six navigational purposes is not only the cost, but also the processing time. For example, to cover the full extent of a coastal chart at the scale 1:150 000, it would require around 100 high resolution images, but only one or two medium resolution images. Based on the mapping requirements, the medium

resolution (Sentinel-2 and Landsat) imagery also exceeds what is needed to meet mapping standards for coastal scale. Since the data from these sensors is free of charge, and the large swath size of one image is often enough to cover the full chart, it is preferred to use the medium resolution data over the lower resolution data. The medium resolution imagery also provides a suitable level of positional accuracy. For these reasons CHS does not use low resolution data for shoreline mapping.

**Table 2** : Electronic Navigational Charts (ENC) scales based on Navigational Purpose (IHO , S-66, 2018)

Navigational Purpose	Name	Scale Range	Required Image Resolution
1	Overview	<1:1 499 999	Low
2	General	1:350 000 – 1:1 499 999	Low
3	Coastal	1:90 000 – 1:349 999	Medium
4	Approach	1:22 000 – 1:89 999	Medium
5	Harbor	1:4 000 – 1:21 999	High
6	Berthing	> 1:4 000	High

The use of optical imagery requires cloud-free data. Alternatively, microwave remote sensing using Synthetic Aperture Radar (SAR) overcomes these limitations by offering valuable geophysical parameters with a high frequency revisit in all-weather and daylight-independent conditions. The acquisition in ascending and descending orbits also helps in targeting acquisition times that correspond with the low and high water lines.

### 3. Methods

#### 3.1 Optical Satellite derived Bathymetry (SDB)

One of the main study sites used to develop the CHS SDB approach was Cambridge Bay (69°07' N, 105°02' W), a hamlet located on Victoria Island, Nunavut (**Figure 1**). Water in Cambridge Bay is generally clear with a depth visibility of around 15 m. The bottom is mostly composed of sand and rock, but the benthic environment is more heterogeneous with numerous patches of vegetation, making the site somewhat complex for SDB.

**Figure 1.** Location of the Cambridge Bay study site on Victoria Island, Nunavut.



### 3.1.1 Sensors

Prior to defining the best approach to use for the study, a major step was to evaluate the impact of the EO datatypes on the accuracy of SDB (Ahola et al. 2018). CHS follows the guidelines (**table 3**) based on the International Hydrographic Organization (IHO) CATegory of Zones Of Confidence (CATZOC) levels to define the acceptable standard of data (International Hydrographic Organization , S-57 Supplement, 2014).

**Table 3** : Required depth accuracies for IHO CATZOC levels (IHO, 2014).

CATZOC Level	Depth Range (m)	Required Depth Accuracy ( $\pm$ m)
A1	0-10	0.6
	10-30	0.8
A2 & B	0-10	1.2
	10-30	1.6
C	0-10	2.5
	10-30	3.5

The sensors that were tested to evaluate the best option for use in optical SDB were: WorldView-2, Pléiades, PlanetScope, SPOT, Sentinel-2, and Landsat-8. Table 4 provides an overview of the specifications of the imagery provided by each sensor. To simplify the analysis of sensor impacts on SDB, the Lyzenga's empirical linear multi-band SDB technique (Lyzenga, 1985) was selected as the only approach used to extract the SDB.

**Table 4** : Specifications for satellite imagery examined for this work.

Sensor	Acquisition Date	Acquisition Time (UTC)	Sun Azimuth Angle ( $^{\circ}$ )	Sun Elevation Angle ( $^{\circ}$ )	Spatial Resolution (m)
WorldView-2	20 September 2015	18:37	176	22	2
Pléiades	12 July 2016	18:52	175	43	2
PlanetScope	10 July 2017	17:56	159	42	3
SPOT	1 August 2015	18:35	170	39	6
Sentinel-2	11 August 2017	18:59	179	36	10
Landsat-8	28 August 2015	18:37	173	31	30

The SDB results that each sensor produced were compared with the IHO CATZOC requirements (**Table 3**). In this study, we did not consider the S-44 (S-44 is one of the IHO series of hydrographic standards) as the data was already available to be used for chart production. The SDB results demonstrate that the spatial resolution has an impact on the SDB accuracy as seen by the correlation in **Figure 2**, with higher resolution data generally outperforming low resolution sensors for overall accuracy. PlanetScope presents an exception to this trend, as it achieved worse



results than lower resolution SPOT data. This may be due to reduced positional accuracy (relative to the other sensors) and reduced calibration potential with the microsatellite format. Based on these results, the low-resolution Landsat-8 and Sentinel-2 datasets should not be used as the main sensors for charting purposes but could be useful tools for mission planning. The PlanetScope data also did not achieve adequate results in the deep water and was outside the CATZOC B requirement for the 0-10m range. The two high resolution sensors (WorldView-2 and Pléiades) provided the best results and therefore are the main sensors used by CHS for SDB chart updates. Even if the study clearly demonstrates a link between the sensors spatial resolution and the SDB accuracy, it is important to note that the different acquisition dates of each image limit our understanding of spatial resolution impact on the SDB accuracy. The suitability of the best image to use for SDB also depends on other factors such as sun glint effect, water turbidity, sun angle, waves and cloud coverage.

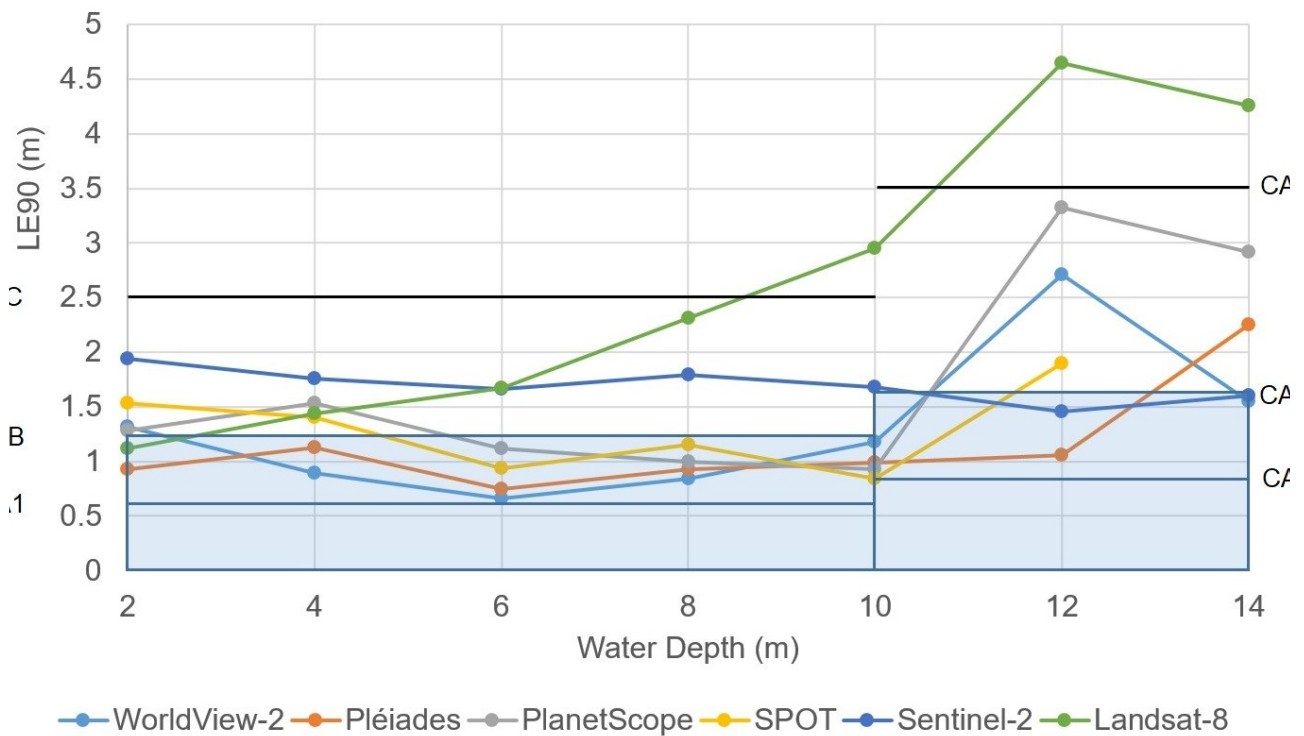


**Figure 2.:** SDB accuracy based on sensor type, and IHO requirements based on water depth. The shaded blue boxes represent the IHO CATZOC A/B requirement based on water depth.

3.1.2 Spectral bands

Besides the spatial resolution, there are other important factors to consider when selecting the best image to use. Another study by CHS (Chénier et al. 2018) demonstrated that the radiometric resolution of a sensor also has an impact on the SDB accuracy. The lower frequency wavelengths such as the yellow and red bands of WorldView 2 and 3 help improve the SDB accuracy in shallow waters (0-4 m). Therefore, the technique used should utilize the advantage of different bands offered by multispectral sensors. The results in Chénier et al 2018, demonstrated that in the two empirical approaches tested ; the Multi-Band Model (Lyzenga,1985) and the band ratio model (Stumpf et al. 2003), the multi-band approach generally exceeded the performance of the band ratio technique with the traditional blue and green ( $\ln(B)/\ln(G)$ ) band ratio. By adapting the band ratio approach with different band ratio combinations (Chenier et al. 2018) based on water

depths, the results achieved were almost identical to that of the multi-band technique. The blue and green band ratio is very effective for sites that have clear, deep waters, but for shallow environments with higher sediment levels, the blue and yellow band ratio provided better results. Thus by adapting the band ratio combination approach to the site conditions and water depths, the accuracy of the SDB will increase.

### 3.1.3 SDB approaches

After determining the optimal sensor to use, CHS evaluated different SDB approaches that would provide the best results in Canadian waters. During this work, CHS was the first to propose looking at photogrammetric approaches to extract SDB (Chénier et al., 2016). Two photogrammetric approaches were evaluated: an automatic approach (Hodul et al., 2018) and the traditional 3D manual approach (Chénier et al., 2018). Other techniques like classification and empirical approaches were also tested. Since all the approaches provided different advantages and disadvantages, optimal results were obtained by developing a hybrid model that leverages the advantages of the different approaches and also meets the level of confidence in the SDB. Using a level of confidence approach (Chénier et al., 2019a), CHS was the first HO to obtain the CATegory of Zones Of Confidence (CATZOC) A2/B requirement for SDB. The proposed level of confidence method operates through understanding the level of agreement between each of the applied SDB techniques. It aims to develop a final SDB estimate where the highest number of techniques agree within 1 meter. **Table 5** provides the results obtained by using the level of confidence approach. The area where at least three of the four techniques agreed represent 81% of the SDB coverage. These results not only provide confidence to the results, but also match the CATZOC A2/B requirements (**Table 3**), and therefore could be used as a tool to update nautical charts.

**Table 5.** Accuracy assessment results for the multi-approach technique.

Number of Techniques Agreeing within 1 m	LE90 (m)								
	Coverage %	Bias	Depth Range						
			0-10	0-2	2-4	4-6	6-8	8-10	10-14
4	31	-0.10	1.01	1.21	0.85	0.85	0.98	1.27	1.00
3	50	-0.19	1.26	1.23	0.90	1.14	1.28	1.25	1.24
2	19	0.05	1.28	1.30	1.21	1.25	1.24	1.07	1.90
4 & 3	81	-0.16	1.21	1.26	0.87	1.08	1.24	1.28	1.20
All	100	-0.12	1.24	1.30	0.95	1.15	1.24	1.18	1.78

## 3.2 SAR Bathymetry

As demonstrated above, the optical SDB bathymetric measurements of shallow water are hampered by the water clarity. The accuracy tends to decrease with water depth and in Canadian waters, visible depth range is limited to around 20 m. SAR bathymetry can provide estimates based on the influence of underwater structures on hydrodynamic processes by taking advantage of the high sensitivity of radar backscatter of rough surfaces. In the following section, we present a review of results obtained based on investigating and developing SAR applications.

The ocean's surface, gravity, waves and water depth are related by the linear dispersion relationship in shallow water (Brusch et al. 2011; Mishra et al. 2014). This relationship is used to estimate the bathymetry in near coastal waters. Particularly when approaching the coast, waves and



seabed change rapidly in a coordinated manner (Wiehle and Pleskachevsky 2018). The waves tend to align parallel to the shoreline and manifest by an increase in both height and frequency as a response to changes in the underwater topography (Brusch et al. 2011). SAR wavelengths of the observable long gravity wave changes can be extracted using Fast Fourier Transform (FFT) and Wavelet transform methods on high-resolution SAR imagery (Mishra et al. 2014). Limitations of these methods stem from finding adequate SAR data with discernable wave features, and the quality and accuracy of these methods remain largely unconstrained as the studies investigating them are limited to very high-resolution imagery. CHS, in collaboration with C-CORE tested the SAR bathymetry approach using a study site on the north shore of Haida Gwaii Island, British Columbia (BC). In this study, four Sentinel-1 images with visible waves were selected and used to generate the SAR SDB. The acquired images are Ground Range Detected (GRD) products with Interferometric Wide Swath modes and have a nominal 10 m resolution in VV polarization (**Figure 3**).

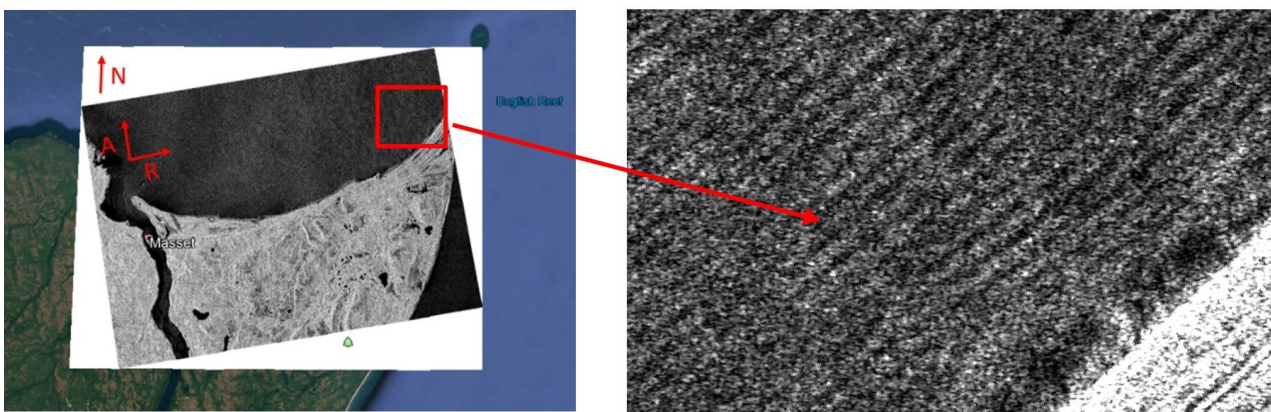


**Figure 3** : Sentinel-1 scene of Haida Gwaii with a zoomed in view of waves visible in the image (C-CORE, 2019).

The retrieval process performance assessment was performed using CHS surveys (C-CORE, 2019). **Figure 4b** shows a relative agreement of estimated SAR bathymetric values against single beam CATZOC B survey data 4a. With a combined RMSE of 4.49 m which indicates that the SAR bathymetry does not meet the IHO CATZOC requirement for charting purposes (**Table 3**). By investigating the different water depth classes (Table 6), we noticed that as with optical SDB there is a correlation with water depth an accuracy, with accuracy tending to decrease as depth increases. These results demonstrate that SAR SDB can meet the CATZOC C requirement for water depth from 10 to 40 m. Even if the main goal of this study was to demonstrate that SAR SDB could be used for mission planning and shoal detection, the accuracy obtained in the 10-40 m also demonstrated potential for chart update. There are also several other factors that can impact SAR bathymetry results. We can cite the quality of surveys data, the spatial resolution and the frequency of the SAR system used, the difference of water height to the sea level during the acquisition and the quality of the wave features present in imagery. However this technique offers other advantages to CHS. Water depths of 40 m could be extracted in the Haida Gwaii site where optical SDB could only reach depths of up to 10 m. The main limitation of this technique is that the user must have suitable imagery. The approach requires one or more SAR images capturing discernable wave features on sea surface. As the measured SAR backscatter from surface water is dependent on surface roughness. Changes in surface wave properties are induced by changes in the topography of the sea bottom. Therefore, the latter can be sensed through its effects on sea surface. Throughout the study, 58 images were investigated with only four of those images being usable to extract the SAR SDB. Due to this limitation, no images were available for the Cambridge Bay site. Further investigations are also needed to

assess the approach using Radarsat-2 and RADARSAT Constellation Mission (RCM) data acquired in higher spatial resolution modes, as better resolution data could help improve the accuracy of the SAR SD

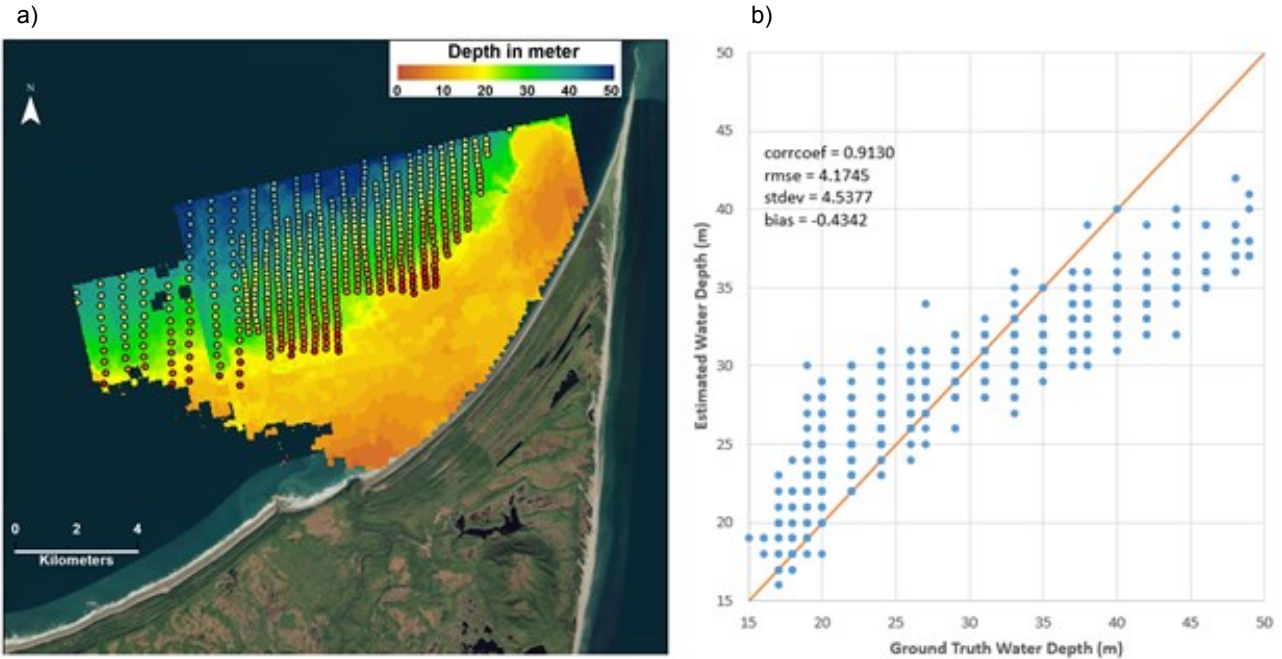


**Figure 4 a) & b) :** Bathymetry results from the combined average of four Sentinel-1 scenes acquired on 14 Dec. 2018, 19 Dec. 2017, 12 Nov. 2017, and 8 Oct. 2017, respectively. In (a), single beam CATZOC B survey data dispalyed on the top of estimated bathymetry and in (b), the chart of estimated water depth against survey data. ©ESRI Imagery Basemap

**Table 6** below breaks down the RMSE values by depth class for each image as well as the combined average of all images. Results indicate that depths up to 40 m output predicted depths with RMSE values ranging from 3 to 5 m. However, above 40 m in depth the error significantly increases to more than 8 m. This suggests that SAR bathymetry can only be used in intermmediate depths as seen in **Figure 4** as well.

**Table 6 :** RMSE values by range depth of the four Sentinel-1 scenes as well as a combined average of all four images.

Depth Range (m)	Average		Image 1		Image 2		Image 3		Image 4	
	No. of Points	RMSE (m)	No. of Points	RMSE (m)	No. of Points	RMSE (m)	No. of Points	RMSE (m)	No. of Points	RMSE (m)
10-20	99	3.40	87	4.61	80	3.31	85	3.98	90	5.24
20-30	266	3.25	237	4.58	193	3.41	217	3.40	245	5.05
30-40	146	3.67	118	3.11	68	5.18	104	3.66	132	3.03
40-50	94	8.39	65	7.99	9	8.78	43	9.27	87	7.62
<b>0-50</b>	<b>605</b>	<b>4.17</b>	<b>507</b>	<b>4.68</b>	<b>350</b>	<b>3.87</b>	<b>449</b>	<b>4.13</b>	<b>554</b>	<b>5.00</b>

### 3.3 InSAR technique for VIRTUAL Tidal GAUGES

Making accurate and up to date predictions of water levels is critical to ensure safe navigation. Currently the Canadian Hydrographic Service (CHS) is relying on traditional physical water level gauges to create tidal predictions. While some regions have an even distribution of water gauges,



other areas like the Canadian Arctic suffer from limited spatial coverage. There are only 5 permanent water gauges in the Arctic to cover an area close to 4 million km<sup>2</sup>. The aim of this study is exploring the potential of Interferometric Synthetic Aperture Radar (InSAR) to extract water level information and help charting coastal areas (Chénier et al., 2020a).

To test the approach, a study site with large tidal variations (up to 12 m) and shallow slopes was selected in the Canadian Arctic. The study site is located in Hopes Advance Bay on Ungava Bay, QC (**Figure 5**). Five datasets were acquired for this region: Two co-registered Bistatic TanDEM-X/TerraSAR-x single look slant range complex SAR images (CoSSC), collected on September 22, 2012, were used for the creation of the InSAR DEM. The images were acquired with a right-looking ascending pass in HH polarization. For the low water line, a Worldview-3 image was acquired on October 2, 2017. For the medium water line, a PlanetScope image acquired on July 25, 2015 was used. To extract the high water line, a RADARSAT-2 image in fine mode was used with an acquisition date of September 8, 2015. The validation data were from tidal gauge observations obtained from existing station number 4325 (**Figure 5**) located at Hopes Advance Bay.



**Figure 5** : Hopes Advance Bay Site, Ungava Bay , Northern Québec, Canada. Image © Service Layer Credits: ESRI, Garmin, GEBCO, NOAA NGDC, and other contributors.

The InSAR processing of the Bistatic TanDEM-X/TerraSAR-x images was performed using the GAMMA software, and the DEM was generated with a 4 m pixel grid. Before comparing with the tidal gauge information, the model is adjusted to the Chart Datum (CD). **Figure 6** represents the InSAR DEM generated from the TanDEM-X/TerraSAR-X images overlapped with the coastline extracted from the imagery at the varying water levels (low, medium and high). Since the water line is very close to a level line, a mode technique was used to extract the most common values from each of the lines. This technique removes the errors generated in the InSAR model. Before comparing the tidal gauge information and InSAR DEM values at the water lines, the values need to be corrected to the CD. The most commonly used CD by CHS for tidal waters is the lowest low water at large tide (LLWLT). The LLWLT values are calculated by averaging the lowest water level from each year for 19 years (Fisheries and Oceans Canada). **Figure 7** represents the formula used to transfer the value from the InSAR DEM to the CD at the LLWLT.

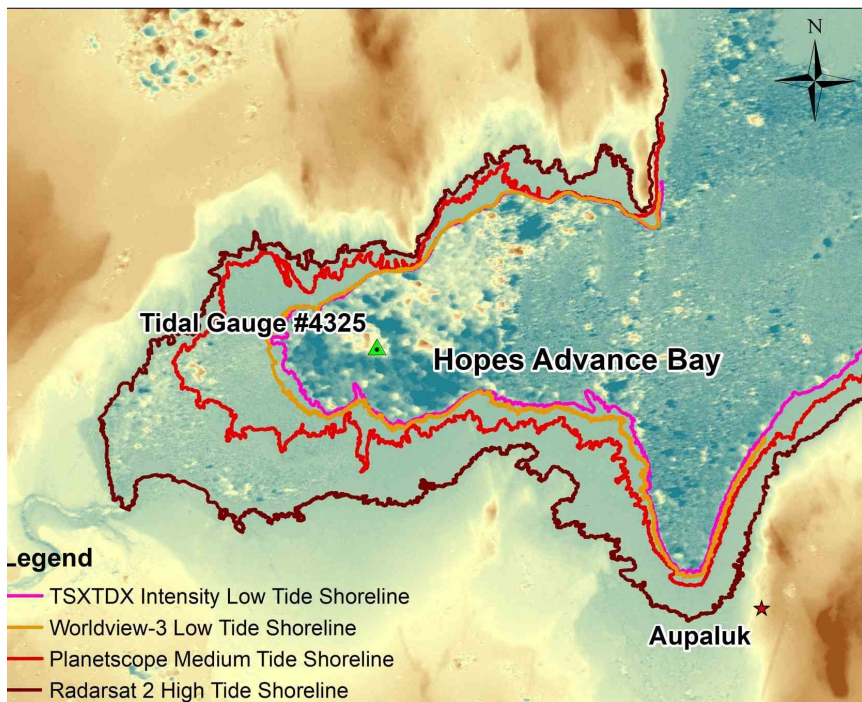


**Figure 6** : Shorelines extracted from the satellite imagery at high (orange), medium (green), and low (yellow and red) tidal conditions are displayed on InSAR DEM generated with Bistatic Tandem-X/TerraSAR-X Single-Look images.

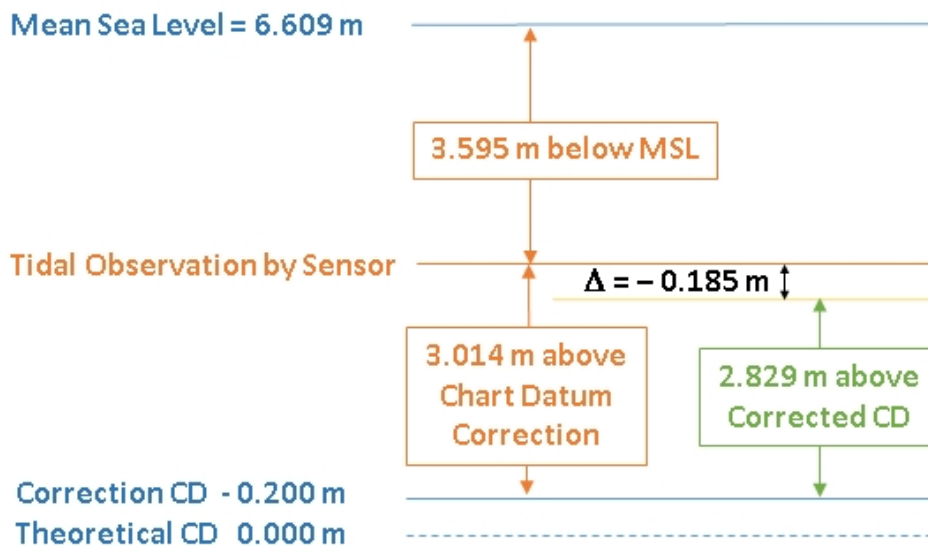


**Figure 7** : Formula used to correct the InSAR values to the CD. Example for the TSX/TDX Intensity image.

**Table 7** provides the results obtained by taking the mode of the InSAR DEM values along the shoreline and subtracting it from the tide station values corresponding to the dates and times of the satellite image acquisitions. The accuracy of the tidal gauge is around 20 cm, therefore the results obtained (27 cm) are within the range of the tidal gauge error. This suggests that the InSAR technique with the coastline extracted from different high-resolution satellite images could

be used as virtual tidal gauges. The results demonstrate a correlation with the errors and tidal conditions, where the best and worst accuracies are seen in low and high tide conditions respectively. Further studies will be required to better understand the source of these correlations, but they could be related to the uncertainty of the tidal gauge which is amplified with large tides. For the InSAR DEM, the reasons explaining this correlation are unknown as there are no large variations in slope or phase coherence. Some of those error could be explained by the different sensor being used to capture the different water lines. More testing will be done to better understand the impact of each sensor on the results. Since there is uncertainty in the tidal gauge and correction of the InSAR to the CD, a relative accuracy assessment was done between each tidal condition (**Table 8**). Even if the results are in the range of the tidal accuracy, the relative accuracy is a good indicator to better understand the error propagation. Besides the low tides of the TerraSAR water line, all of the other results are around 10 cm. This is caused by the overestimation of the water level in the InSAR model, where all the other values at the different tide conditions are lower than the water gauge. This larger error of 47 cm can be caused by the fact that the low water from the InSAR DEM is at the at the limit of water on land and therefore has a lower phase coherence.

**Table 7** : RMSE of the InSAR DEM at different tidal conditions based on shorelines extracted from satellite imagery.

Sensor	Tidal Condition	Tide Station obs (m)	InSAR DEM Mode (m)	$\Delta$ difference Tide Gauge InSAR DEM Elevations (absolute Value)
TSX/TDX Intensity	Low	2.829	3.014	0.185
Worldview -3	Low	4.386	4.164	0.222
PlanetScope	Medium	5.592	5.254	0.338
Radarsat-2	High	7.352	6.990	0.366

**Table 8** : Relative accuracy between different tidal condition.

Tidal Condition	Tidal Condition	Relative difference Tidal Station	Relative difference from InSAR	$\Delta$ difference
Low TerraSAR	Low WV-3	1.55	1.15	0.47
Low WV-3	Med Planet	1.20	1.09	0.11
Med Planet	High Radarsat	1.76	1.74	0.02
High Radarsat	Low WV-3	2.96	0.36	0.14

Virtual tidal gauges (VTG) are also created by extrapolating the data collected from existing tidal gauges using regression models (Xu, 2015a,b). The advantages of the regression models are that they can predict water level at all hours, whereas temporal data collection is the main limitation of the InSAR approach. The primary advantage of the InSAR VTG however is that it is based on up-to-date data, which is especially important in areas that have significant coastal erosion. By combining the InSAR approach with a prediction model, the InSAR VTG could help validate the data that are extrapolated from the regression model. There are other hydrographic applications that could also benefit from the output used to create those VTGs. For example, The



InSAR model, combined with the various contour lines could be used to create dynamic navigational products in the S-100 standards. The up-to-date coastal water line could also be used to support the work on the Continuous Vertical Datum for Canadian Waters (CVDCW).

The introduction into the current workflow of the Ice, Cloud and land Elevation Satellite-2 (ICESat-2) data in order to assist in the estimation of tidal height levels in remote areas has also been considered for future InSAR derived DEM data validation purposes. The Icesat-2 satellite provides along-track heights above the ellipsoid data covering ground and vegetation canopy surfaces and also ice, sea ice, ocean surface height surfaces as well. The ATL08-ATLAS/ICESat-2 L3A Land and Vegetation Height dataset products are acquired by the Advanced Topographic Laser Altimeter System (ATLAS) instrument on board of the ICESat-2 and are processed in fixed 100 meter segments with a temporal resolution of 91 days and variable spatial resolution.

**Figure 8** below shows a swath containing ICESat-2 data compared with the InSAR derived Digital Elevation Model. A height difference of 76 cm is observed at the ICESat-2 point location validating the accuracy of the InSAR derived DEM when compared with the Geodetic data points as a first reference. The drawback of ICESat-2 data is that it only covers a narrow swath of points.

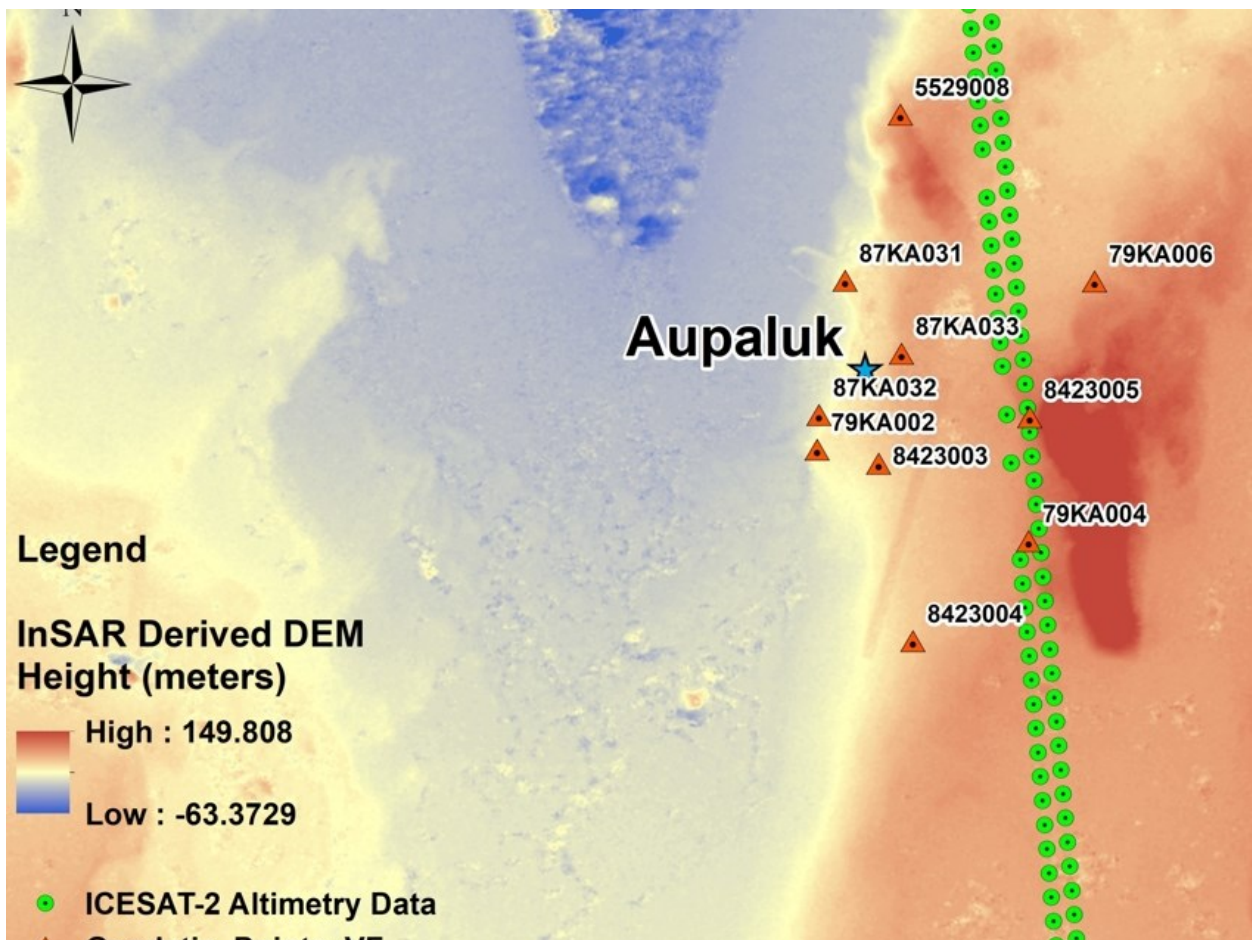


*Figure 8 : Swath covered by ICESat-2 L3A Land and Vegetation Height data*



### 3.4 Shoreline detection

One of CHS's main operational hydrographic applications using EO data is the production of new shorelines for chart updates. In order to best capture the advantages offered by different sensors, CHS developed a hybrid approach that combines radar and optical EO data (Chénier et al., 2019b). For areas with intertidal zones, CHS has developed an approach where the EO data acquisitions are synchronized with the low water levels from CHS's tidal predictions (Chénier et al., 2016). In fresh water systems, the low and high water lines are extracted using monthly averages (Chénier et al. 2019b). The usage of radar data like RADARSAT-2 and RCM is beneficial for capturing low water conditions during periods of high cloud cover (predominantly October to December), thus ensuring that shorelines representing the lowest water level possible are mapped.

#### 3.4.1 Automatic Approach

In order to make the shoreline extraction as automated as possible, the extraction was accomplished through an object-based image segmentation process using eCognition software. Both radar and optical images were used for image segmentation and classification. **Figure 9** represents an area of the Mackenzie River where significant changes were noticed with EO data. The arrow seen in **Figure 9** highlights an area of change in the river's channel, where the full width of the river currently passes through an area of land indicated on the chart.

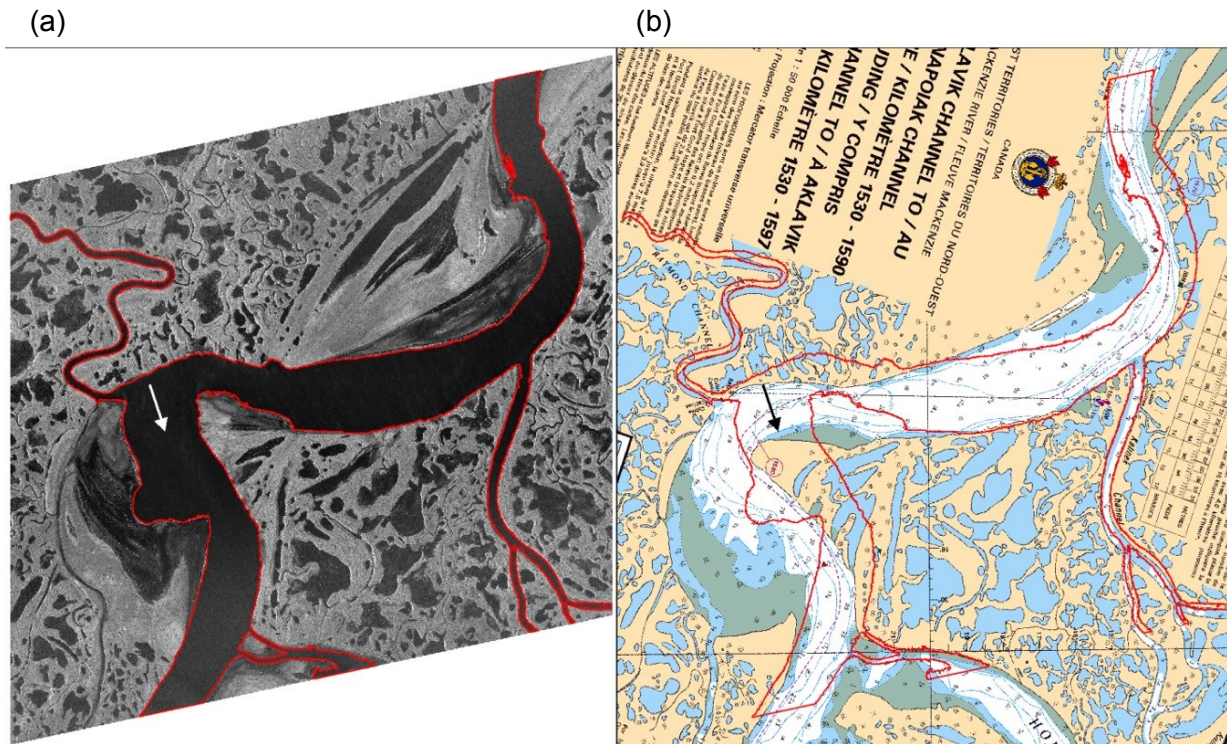


**Figure 9** : Shoreline extracted from EO data over the Mackenzie River. New shoreline overlapped on the RADARSAT-2 Spotlight image (a) and chart 6428 (b). Note the arrow on both maps: on map (a), the arrow is situated near the current centre of the main Mackenzie River channel. In (b), chart 6428 indicates an area of land at the same location. The charted land area spans nearly the entire width of the current river's location at this point. These graphics highlight significant changes in the position of the river since the creation of chart 6428. RADARSAT-2 Data and Products © MacDonald, Dettwiler and Associates Ltd. (2014/2016) – All Rights Reserved. RADARSAT is an official mark of the Canadian Space Agency.

CHS is also exploring automatic methods for shoal detection using artificial intelligence (AI) (Chénier et al., 2020b). Currently, there are large gaps in survey data where potential hazards to navigation are uncharted on CHS products. Using SBEO data, machine learning and deep learning techniques can be applied to identify shoals which may present a hazard to navigation. CHS conducted a test using a random forest (RF) classification which is a machine learning approach, and a convolutional neural network (CNN) classification which is a deep learning approach, over two sites in the Canadian Arctic. The techniques were also tested using both WorldView-2 (2m resolution) and Sentinel-2 (10m resolution) imagery to understand if spatial resolution plays a significant role in classification accuracy. Across the two sites, overall accuracies ranged between 79-85% for both techniques and sensors. These results indicate that neither method is superior. The RF classification is much faster and more user-friendly, but the model cannot be applied to just any image. The CNN classification requires a large training dataset and requires more time and computing power to train the model and classify the image, but it can be built to identify shoals in any image of the same sensor which would be beneficial for CHS in the long-term.

#### 3.4.2 Rate of change

A second aspect of the project is to evaluate the rate of change on the river to better understand the frequency at which the chart would need to be updated. As illustrated in **Figure 10**, by using archived Landsat data ranging from 1972 to 2011 and a Sentinel-2 image from 2018, a rate of change of approximately 220 m per decade was determined in the most dynamic areas within chart 6428. The rate of change was calculated by measuring the maximum distance from the vectors of the shoreline extracted from the 1972 and 2018 images. For this 46-year period, the maximum distance between the two vectors is approximately 1 km, which represents close to 22 m of change per year. To better predict future changes in the river, data for every decade (1972 to 2018) were also estimated. This approach is needed to ensure that the shoreline changes were not introduced by one major event, such as a landslide, and progress consistently. Based on the extracted shorelines, we can see in **Figure 10** that although some decades, 1982 to 1992 for example, exhibit more change, there is a gradual shift in the river shoreline throughout each decade. Therefore, we can deduce that this general trend will continue to occur in the future and thus special attention will be required in those areas of the river to ensure that the charts are up to date. The detail at which a cartographer can update a map/chart is half a millimeter at chart scale. The scale of chart 6428 is 1:50,000; as such, 0.5 mm on the chart represents 25 m on the ground. With a rate of change of approximately 22 m/year, this chart would need to be reevaluated at least every 2 years.

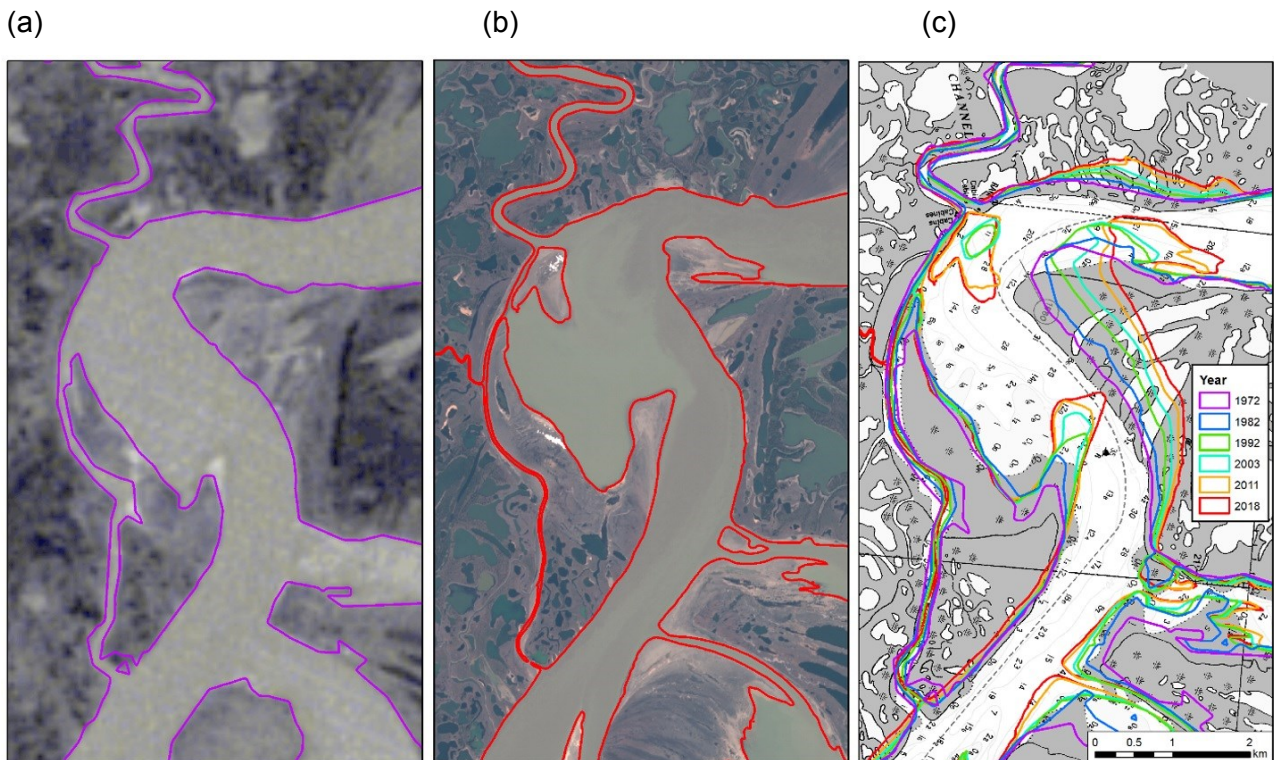


**Figure 10** : Segmentation results showing extracted main Mackenzie River channel and tributaries over a Landsat image from 1972 (a), a Sentinel-2 image from 2018 (b) and over chart 6428 (c). Imagery © 1972, U.S. Geological Survey and © 2018, Copernicus.

### 3.5 Polarimetry for intertidal zone mapping

Radar EO data can offer many advantages such as collecting data in conditions of full cloud cover. The polarimetric capabilities of SAR can help in identifying intertidal zones, which are important to CHS since variations in water level can have impacts on the safety of navigation, and therefore the intertidal zones must be mapped on CHS charts.

In intertidal zones, the contrast between target elements is based on their differences in dielectric properties, and the structure of both soil (e.g. soil moisture and roughness, sediment size and shape) and vegetation (e.g. size, orientation and shape) can be used as a contrasting mean for an enhanced sediment classification (Gade et al., 2008). Polarimetric SAR data has been investigated for surface roughness characterization and mapping intertidal zones (Park et al., 2009; Souza-Filho et al., 2011; Lee et al., 2012; Geng et al., 2016; Gade et al., 2018). In contrast to single or dual-polarizations, the use of polarimetric parameters enhance the discrimination of different types of target objects based on their scattering responses (Lee et al., 2012, 2009; Boener et al., 1998; Touzi et al., 2020).

Recent studies investigate the use of polarimetric parameters generated from Quad-pol Radarsat-2 data and the potential of Compact Polarization (CP) of the RCM mission from simulated parameters (Omari et al., 2020). **Figure 11** shows an example of these parameters and their equivalent classification results using a Random Forest (RF) approach over a study area located near the village of Tasiujaq (58°42' N–69°56' W) along the banks of the Baie aux Feuilles at the mouth of the Bérard river on the west side of Ungava Bay.



In the upper three figures, (a) presents the Freeman-Durden (FD) decomposition, (b) the Touzi discriminators using the Quad-pol images and (c) the Raney m-delta classification derived using the CP. In **Figure 11(a)**, the double-bounce is shown in red, volume scattering in green, and surface scattering in blue. The vegetation (green area) is dominant over land (FD\_volume) whereas in intertidal areas (pink), a mixture of FD\_volume and FD\_double-bounce. **Figure 11(b)**, displays a color composite of Touzi extrema represented by a combination of maximum and minimum values of the degree of polarization and the scattered wave intensity (pmin in red, pmax in green and R0max in blue). Land vegetation is highlighted with the blue color where R0max is dominant, exposed rocks represented in white color and intertidal zones in yellow (contribution of both pmin and pmax). The m-delta presentation on the other hand, shows the potential ability to discriminate exposed rocks and open water. Difficulties of discriminating the latter in both FP presentations rise in localized areas where the water surface is affected by wind and wave conditions (surface water is rougher).

Classification results of polarimetric parameters are also shown in **Figure 11 (bottom three images)**. The Random Forest classification output of FP Freeman-Durden (FD) parameters, Touzi discriminators (pmin, pmax, R0max) extrema of the DoP), and m-delta parameters show an overall accuracy ranging between 61% to 71% (Omari et al., 2020). The polarimetric parameters (information) tend to provide a better description of geophysical properties of the surface and account for roughness, biomass and soil moisture variables. The obtained results from the Omari et al., (2020) study demonstrated that the use of only one polarimetric decomposition as a sole source of information to feed the classification process can provide acceptable results. The authors suggested that to further enhance the accuracy, the polarimetric decomposition must be complemented with another type of data such as optical imagery. This approach is challenging as both data types have to be acquired simultaneously to illustrate identical tidal conditions. This can prove to be quite complicated as the changes in tidal water content of the study site (wet vs dry) and its winding channels are controlled mainly by tidal elevation in intertidal areas. Moreover, the reported results in Omari et al., 2020, showed that fully polarimetric parameters provide the best accuracy due to their high sensitivity to varying surface types. The classification using simulated RCM CP parameters appears slightly less accurate. Still, the CP m-delta obtained results are reasonable when taking the complex and challenging environment into account. The large swath of the CP can encompass the relatively small decrease of classification accuracy compared to FP results, and potentially be used for large scale mapping and monitoring purposes. This may be true for current missions such as ALOS-2 and RCM but a new generation of upcoming satellite SAR missions will be equipped with digital antenna beams offering fully polarimetric capabilities with high resolution and larger swaths.

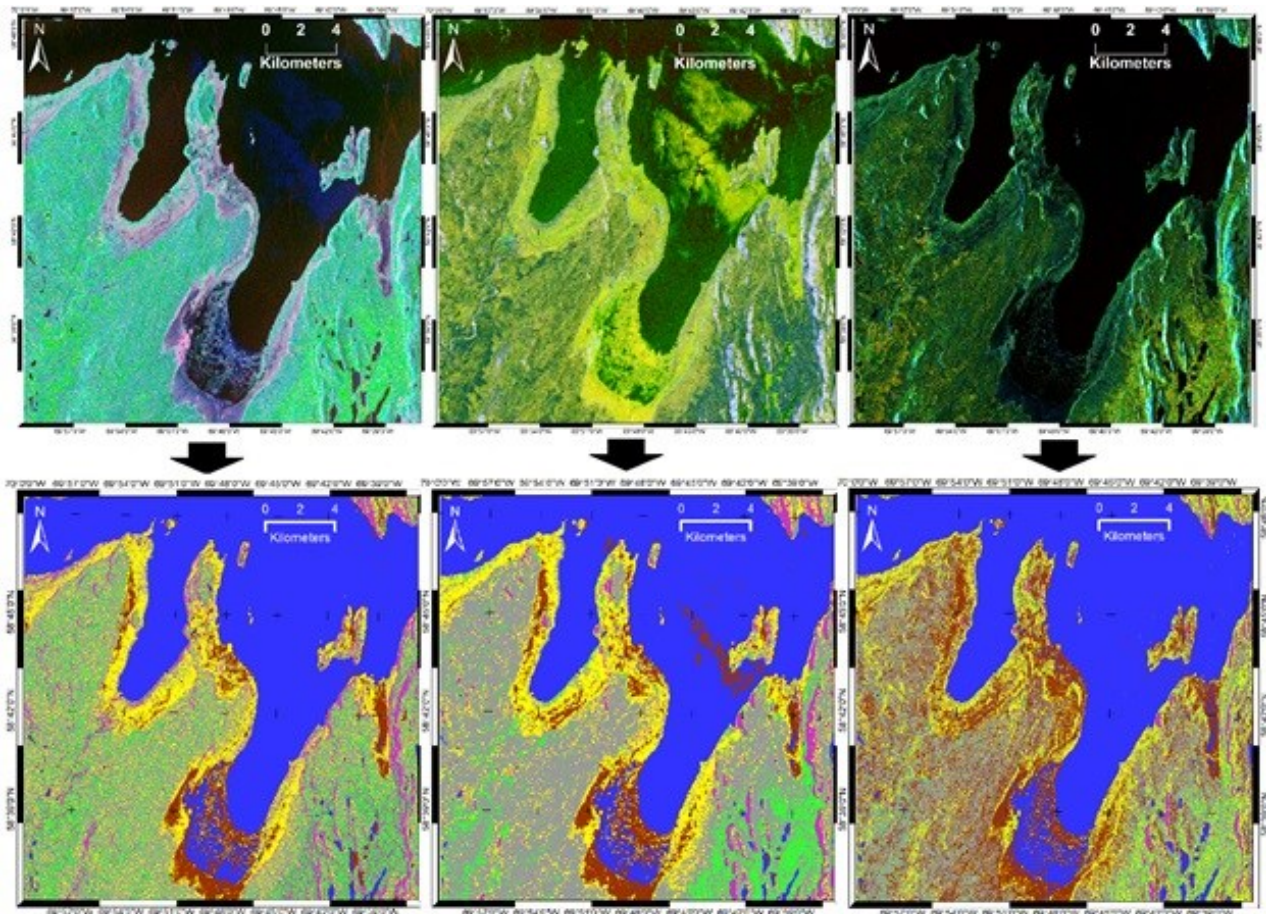


**Figure 11:** Radarsat-2 scene and equivalent Classification results using Random Forest approach over a study area located near the village of Tasiujaq. (a) FP polarimetric Freeman-Durden decomposition (red: double bounce, green: volume scattering and blue: surface scattering), (b) RGB composite of Touzi extrema parameters (red:  $P_{min}$ , green:  $P_{max}$  and blue) and (c) is the CP Raney  $m$ -delta classification

#### 4. Discussion

Some recently developed techniques, such as polarimetry for intertidal zone mapping will be integrated in the techniques already in operation like the automatic shoreline detection procedure. This will help reduce the physical component of shoreline extraction and will improve the overall accuracy by reducing human error.

Other EO applications that leverage pre-existing data products have also been developed at CHS. An example of these applications assess water clarity for the planning of LiDAR and imagery acquisitions. Determining the best time of the year to plan LiDAR survey and imagery acquisition is critical to ensure a high level of quality in the data. Avoiding critical dates for alga bloom and sediment deposits will optimize the quality of the data and will reduce the cost of the survey. One of the datasets used by CHS to help plan data acquisition is the MODIS Diffuse Attenuation coefficient for downwelling irradiance at 490 nm ( $K_d$  490) Level 3 data. The Modis  $K_d$  490 products have a 4km resolution but they provide a good indication of the best time of the year to collect data. Research and development is underway to improve mission planning and develop better accuracy in coastal areas. The  $K_d$  489 can be calculated from high resolution data like Sentinel-3A OLCI (300 m resolution) and Sentinel-2 (60 m resolution). In this top-down approach, the lower resolution data are used to target the key dates for the data acquisitions and afterward, the higher resolution data are used to calculate the water clarity in the key periods identified by the

KD 490 obtained from the MODIS data. For the validation of our products, CHS mainly uses multibeam and LiDAR data, but in areas where data is limited, CHS has been looking at other alternatives for validation such as data from the Advanced Topographic Laser Altimeter System (ATLAS) onboard the Ice, Cloud, and Land Elevation Satellite (ICESat-2).

Some applications developed at CHS can also benefit DFO. For example, the InSAR technique can also be used to predict landslides. In June 2019, a landslide along the Fraser River north of Lillooet BC, took place causing big pieces of rock to fall into the river, obstructing the passage of salmon migrating upstream. To prove the suitability of InSAR data processing to monitor the stability of slopes along navigable streams for predicting potential disasters, an interferometric stack of SAR images was used. Upon completion of the InSAR time series analysis, the detection in the progression of displacements over time was analyzed, leading to the identification of the precise location of the landslide incident as shown in **Figure 12(a)**. **Figure 12(b)** shows the InSAR Temporal progression displacement. The displacements (in cm) are displayed on the Y-axis while the temporal line is shown on the X-axis (days). The InSAR temporal chart shows that minor displacements started to appear 60 days into the time series analysis, beginning on March 08, 2019. As further InSAR datasets were ingested and processed, an increasing deformation trend was observed until the final collapse of the rock cliff on day 116 when the incident took place (June 23rd, 2019).

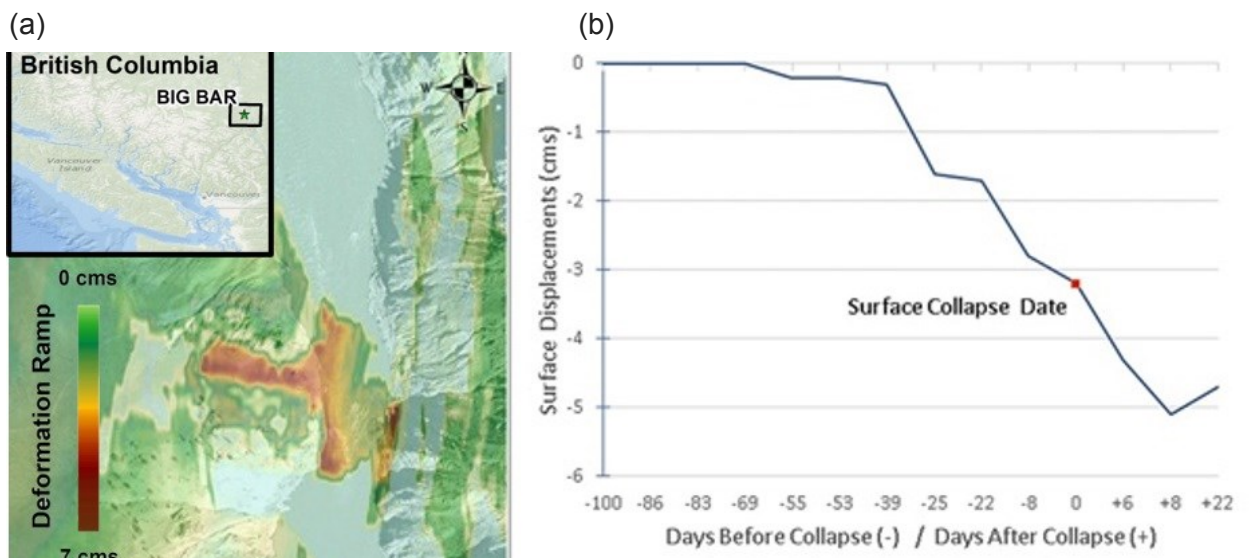


**Figure 12.** (a) Cliff Collapse Location and Deformation Progression Ramp (b) diagram of the collapse in day before and after the collapse day of June 23<sup>rd</sup> 2019.

## 5. Conclusion

As demonstrated in this paper, although different EO techniques can offer many advantages to hydrographic applications, these technologies are still not being utilized at their full potential by HOs. In its specifications of standards, the IHO recognizes the usage of EO in hydrography, however more efforts are still needed to better incorporate EO data. Currently the usage of EO data in official nautical products has been limited. Much of the limited use can be attributed to the lack of qualified expertise in effectively implementing the techniques derived from EO data, as well as the level of confidence which HOs are comfortable in utilizing EO products for hydrographic applications. In order to help accelerate this science, with the support of the IHO, CHS in collaboration with Service Hydrographique et Océanographique de la Marine (SHOM) and the National Oceanic and Atmospheric Administration (NOAA), organized the first International Hydrographic Remote



Sensing workshop (18 to 20 September 2018, Ottawa, Ontario, Canada). At this workshop, 11 HOs were represented and presentations on the different EO applications in hydrography were presented by the HOs, government agencies, members of the private sector as well as representatives from universities. To help the progression of the usage of EO data, a report was presented at the 2nd IHO Council meeting (IHO Council, 2018).

*“It was felt that regional hydrographic commissions should encourage the use of hydrographic remote sensing (HRS) and satellite-derived bathymetry (SDB) imagery should be used daily by Hydrographic Offices to improve chart information and assist in making cartographic decisions”.*

*“ The Secretary-General pointed out the interrelationship between SDB and S-44 and the compelling need to open categories beyond nautical charting surveys, using a metrics approach. The Chair of HSSC gave assurance that HSPT was working on the metrics in liaison with other working groups, especially with respect to data quality. Participants welcomed the excellent report and the use of SDB/HRS, highlighting its value for planning purposes and with respect to highly changeable areas, including in areas with high tectonic activity and islands that were not easily accessible”*

In order to further implement the use of EO data throughout CHS and to help recruit the expertise needed within the organization, a Remote Sensing Center of Expertise (CHSRSCoE) was created in 2017 to apply the EO techniques developed. As previously mentioned, the most common requests are for the creation of new shorelines, but in June of 2018, CHS updated its first chart that has been updated using SDB data (Havre-aux-Maisons, CHS chart 4955, New Edition: 06/15/2018). CHS has also developed processes to include SDB data in future chart production. The RSCoE at CHS will continue developing new approaches that can help leverage the advantages offered by EO data and adapt the developed techniques to the large variety of new sensors and EO products that will become available in the future.

**Funding:** This research was funded by the Government Related Initiatives Program of the Canadian Space Agency and Ocean protection Plan

**Acknowledgments:** The extraction of the isobaths for the manual photogrammetric approach was completed under a contract with Effigis Geo Solutions.

**Conflicts of Interest:** The authors declare no conflicts of interest.

## 6. References

- Ahola, R., Chénier, R., Faucher, M.-A., Horner, B., and Sagram, M. (2018). Satellite Derived Bathymetry for Arctic Charting: A Review of Sensors and Techniques for Operational Implementation within the Canadian Hydrographic Service. In Proceedings of the SPIE 10784, Remote Sensing of the Ocean, Sea Ice, Coastal Waters and Large Water Regions. Berlin, Germany.
- Boerner, W.M., Mott, H., Luneburg, E., Livigstone, C., Brisco, B., Brown, R.J., and Paterson, J.S. (1998), **Manual of Remote Sensing**, 3rd ed., vol. 2, John Wiley & Sons, Hoboken, NJ.
- Bruschi, S., Held, P., Lehner, S., Rosenthal, W., and Pleskachevsky, A. (2011). “Underwater Bottom Topography in Coastal Areas from TerraSAR-X Data”, **International Journal of Remote Sensing**, 32, pp. 4527–43.
- C-CORE. (2019). “Bathymetric Estimation Sentinel-1 Imagery.” Report R-18-056-1494, Revision 1.0.

- Chénier, R., Faucher, M.A., Ahola, R., Jiao, X., and Tardif, L. (2016). Remote sensing approach for updating CHS charts. In Proceedings of the Canadian Hydrographic Conference, Halifax, Canada.
- Chénier, R., Abado, L., Sabourin, O., and Tardif, L. (2017). "Northern marine transportation corridors: Creation and analysis of northern marine traffic routes in Canadian waters", **Transactions in GIS**, 21, pp. 1085-1097.
- Chénier, R., Abado, L., and Martin, H. (2018). "CHS Priority Planning Tool (CPPT)—A GIS Model for Defining Hydrographic Survey and Charting Priorities", **ISPRS International Journal of Geo-Information**, 7, pp. 240-254.
- Chénier, R., Faucher, M.-A., Ahola, R., Shelat, Y., and Sagram, M. (2018). "Bathymetric Photogrammetry to Update CHS Charts: Comparing Conventional 3D Manual and Automatic Approaches", **ISPRS International Journal of Geo-Information**, 7, pp. 395-409.
- Chénier, R., Faucher, M.-A., and Ahola, R. (2018) "Satellite-derived bathymetry for improving Canadian Hydrographic Service charts", **International Journal of Geo-Information**, 7, pp. 306-331.
- Chénier, R., Ahola, R., Sagram, M., Faucher, M.-A., and Shelat, Y. (2019a). "Consideration of Level of Confidence within Multi-Approach Satellite Derived Bathymetry", **International Journal of Geo-Information**, 8, pp. 48-64.
- Chénier, R., Omari, K., Ahola, R., and Sagram, M. (2019b). "Charting Dynamic Areas in the Mackenzie River with RADARSAT-2, Simulated RADARSAT Constellation Mission and Optical Remote Sensing Data", **Remote Sensing**, 11, pp. 1523-44.
- Chénier, R., Blondel, E., and Omari, K. (2020a), InSAR for Tidal Estimation in Support of CVD, Virtual Guages and Dynamic Products. IGARSS Proceeding. Waikoloa, United States.
- Chénier, R., Sagram, M., Omari, K., Jirovec, A. (2020). "Earth Observation and Artificial Intelligence for Improving Safety to Navigation in Canada Low-Impact Shipping Corridors", **International Journal of Geo-Information**, 9, pp. 383-399.
- Fisheries and Oceans Canada. **Vertical Datums**, viewed 22 May 2020, <https://www.tides.gc.ca/eng/info/verticaldatums>
- Gade, M., Alpers, W., Melsheimer, C., and Tanck, G. (2008). "Classification of sediments on exposed tidal flats in the German Bight using multi-frequency radar data". **Remote Sensing of Environment**, 112, pp. 1603-1613.
- Geng, X.M., Li, X.M., Velotto, D., Chen, K.S. (2016). "Study of the polarimetric characteristics of mud flats in an intertidal zone using C- and X-band spaceborne SAR data", **Remote Sensing of Environment**, 176, pp. 56-68.
- Government of Canada. (2017). **Investments under the Oceans Protection Plan to protect Canada's Arctic Coast and Water**, viewed 22 February 2018, [https://www.canada.ca/en/transport-canada/news/2017/08/investments\\_under\\_theoceansprotectionplantoprotectcanadasarcticco.html](https://www.canada.ca/en/transport-canada/news/2017/08/investments_under_theoceansprotectionplantoprotectcanadasarcticco.html).
- Government of Canada. (2015). **World-Class Tanker Safety System: New measures to strengthen oil spill prevention, preparedness and response, and the polluter pay principle**, viewed 28 August 2019, <https://www.tc.gc.ca/eng/mediaroom/infosheets-menu-7672.html>.
- Hains, D. (2020), **What's Hydrospatial?**, International Hydrographic Review, May 2020 Edition, Notes pp.84-93.

- Hodul, M., Bird, S., Knudby, A., and Chenier, R. (2018). "Satellite derived photogrammetric bathymetry", **ISPRS Journal of Photogrammetry and Remote Sensing**, 142, pp. 268–277
- International Hydrographic Organization (IHO) (2014). **S-57 Supplement No. 3 – Supplementary Information for the Encoding of S-57 Edition 3.1 ENC Data**. International Hydrographic Organization, viewed 5 June 2018, [https://www.iho.int/iho\\_pubs/standard/S-57Ed3.1/S-57\\_e3.1\\_Supp3\\_Jun14\\_EN.pdf](https://www.iho.int/iho_pubs/standard/S-57Ed3.1/S-57_e3.1_Supp3_Jun14_EN.pdf).
- International Hydrographic Organization (2018). Facts about Electronic Charts and Carriage Requirements. IHO Publication S-66 – Edition 1.1.0.
- International Hydrographic Organization (2018). 2<sup>nd</sup> Council meeting, London, United Kingdom, [https://iho.int/mtg\\_docs/council/C2/C2Docs.html](https://iho.int/mtg_docs/council/C2/C2Docs.html).
- Lee, J.-S. and Pottier, E. (2009). "Polarimetric Radar Imaging: From Basics to Applications". Boca Raton: CRC Press.
- Lee, Y.-K., Park, J.-W., Choi, J.-K., Oh, Y., and Won, J.-S. (2012). "Potential uses of TerraSAR-X for mapping herbaceous halophytes over salt marsh and tidal flats", **Estuary and Coastal Shelf Science**, 115, pp. 366–376.
- Lyzenga, D.R. (1985). "Shallow-water Bathymetry using combined LiDAR and Passive Multi-spectral Scanner Data", **International Journal of Geo-Information**, 6, pp. 115–125.
- Mishra, M. K., Ganguly, D., Chauhan, P., and Ajai. (2014). "Estimation of Coastal Bathymetry Using RISAT-1 C-Band Microwave SAR Data", **IEEE Geoscience and Remote Sensing Letters**, 11, pp. 671–75.
- Omari, K., Chenier, R., Touzi, R., and Sagram, M. (2020). "Investigation of C-Band SAR Polarimetry for Mapping a High-Tidal Coastal Environment in Northern Canada". **Remote Sensing**, 12(12), pp. 1941–1960.
- Park, S.-E., Moon, W.M., and Kim, D.-J. (2009). "Estimation of surface roughness parameter in intertidal mudflat using airborne polarimetric SAR data", **IEEE Transactions on Geoscience and Remote Sensing**, 47, pp. 1022–1031.
- Souza-Filho, P.W.M., Paradella, W.R., Rodrigues, S.W.P., Costa, F.R., Mura, J.C., and Gonçalves, F.D. (2011). "Discrimination of coastal wetland environments in the amazon region based on multi-polarized L-band airborne synthetic aperture radar imagery", **Estuary and Coastal Shelf Science**, 95, pp. 88–98.
- Stumpf, R. P., Holderied, K. and Sinclair, M. (2003). "Determination of Water Depth with High-Resolution Imagery over Variable Bottom Types", **Limnology and Oceanography**, 48, pp. 547–556.
- Touzi, R., Gosselin, G. and Brooks, R. (2019), **Polarimetric L-band SAR for peatland mapping and monitoring**, ESA Book on Principles and Applications of Pol-InSAR, in press.
- Wiehle, S. and Pleskachevsky, A. (2018). Bathymetry Derived from Sentinel-1 Synthetic Aperture Radar Data. EUSAR 2018; 12th European Conference on Synthetic Aperture Radar, 1–4. VDE.
- Xu Z. (2015a). "The all-source Green's function (ASGF) and its applications to storm surge modeling, part I: from the governing equations to the ASGF convolution", **Ocean Dynamics**, 65, pp. 1743–60.
- Xu Z. (2015b). "The all-source Green's function (ASGF) and its applications to storm surge modeling, part II: from the ASGF Convolution to Forcing Data Compression and A Regression Model", **Ocean Dynamics**, 65, pp. 1761–78.

## 7. Authors Biography

**René Chénier** is a manager at the Canadian Hydrographic service (CHS) where he is managing the Geodesic, Geomatics and Remote Sensing groups. René has been working at CHS for the last 10 years here he has established the CHS Remote Sensing centre of expertise. His fields of expertise include Satellite Derived Bathymetry (SDB), Interferometric synthetic aperture radar (InSAR), Polarimetry, Geometric modeling, Photogrammetry, Radargrammetry, Digital Elevation Model, Classification using artificial intelligence, ship detection and Monitoring, Hydrography, cartography, coastal erosion and habitat mapping.

**Khalid Omari** received the PhD and MSc degrees in remote sensing from the Ottawa-Carleton Geoscience Center, University of Ottawa in 2009 and 2002 respectively. After 14 years as remote Sensing scientist at the Canada Centre for Remote Sensing (CCRS)/Canada Centre for Mapping and Earth Observation (CCMEO), he joined the Canadian Hydrographic Service (CHS) at Fisheries and Oceans Canada (DFO) where he is currently remote sensing scientist developing applying methodologies and approaches of Earth observation generated product related CHS applications. His prior research at CCRS was related to EO applications using SAR polarimetry, Interferometry and optical multispectral/hyperspectral related techniques. His Ph.D. dissertation focused on radiative transfer modeling in vegetation canopies and the extraction of biophysical and biochemical parameters of vegetation canopies from hyperspectral data.

**Enrique Blondel** is a Researcher at the Canadian Hydrographic Service, Fisheries and Oceans department. He graduated as a civil engineer at the Universidad de los Andes (Venezuela) and further studied at l'Université du Québec à Montréal in Geographic Information Systems (GIS). He has 25 years of experience in photogrammetry and remote sensing analyzing and processing synthetic aperture radar imagery for radargrammetry and interferometry applications to generate digital elevation and surficial temporal displacement/deformation models covering natural resources, mining, oil & gas, urban and coastal environments within the Canadian context since 2005; and in the oil and gas field, in the Venezuelan oil industry during the period 1995-2002 in the construction of oil and gas facilities. He has worked for the past 9 years in the research and development of methods with a focus on processing and validation of synthetic aperture radar imagery related to the monitoring and early detection of surficial deformations using interferometric SAR and the generation of InSAR derived digital elevation models in Canada and other countries. Mr. Blondel is furthermore an active landscape photographer enthusiast and deep-sky astrophotography hobbyist.

**Adam Jirovec** has been working at the Canadian Hydrographic Service since 2017, in both the Geomatics and Remote Sensing groups. Adam has over 10 years of GIS and Remote Sensing experience in both a professional and academic setting. He graduated from the University of Ottawa in 2011 with a Bachelor of Arts with a Specialization in Geography, and also holds a post graduate certificate in the Geographic Information Systems program at Algonquin College. His work at the Canadian Hydrographic Service has focused on utilizing Remote Sensing data for charting applications such as coastal mapping, shoal detection and satellite derived bathymetry.

**Mesha Sagram** has been working in the remote sensing group at the Canadian Hydrographic Service (CHS) since 2018 where she has gained much of her experience in remote sensing. Prior to this position, Mesha completed a wide variety of GIS projects through educational and work experience. She has attained a Bachelor of Science degree with Honours in Environmental Science, an Advanced Diploma in GIS Applications, and an Ecosystem

Restoration Graduate Certificate. In the past year, Mesha finished her Master of GIS Applications degree which was focused on improving satellite-derived bathymetry (SDB). Currently, her role at CHS includes research in SDB and deep learning, as well as coastal mapping and shoal detection.